Changes in wave climate off Hiratsuka, Japan, as affected by storm activity over the western North Pacific

W. Sasaki, S. I. Iwasaki, T. Matsuura, S. Iizuka, and I. Watabe
National Research Institute for Earth Science and Disaster Prevention, Tsukuba, Japan

Received 28 September 2004; revised 14 April 2005; accepted 20 May 2005; published 14 September 2005.

[1] Changes in wave climate off Hiratsuka during 1980–2003 are investigated on the basis of hourly observed wave and atmospheric data obtained at a tower 1 km off Hiratsuka in Sagami Bay, Japan. First, the interannual variability of significant wave heights (H_s) for the summer mean (June–August, SH_s) is analyzed. A large difference between wave spectrum ($E(f, t)$) in high SH_s years and that in low SH_s years is found at the frequency of 0.09 Hz. It is revealed that the difference is related to the changes in enhanced tropical cyclone (with central air pressure below 980 hPa) activity in the western North Pacific. Second, the interannual variability of H_s for the winter mean (December–February, WH_s) is investigated. It is found that there is a large difference between $E(f, t)$ in high WH_s years and that in low WH_s years at the frequency of 0.11 Hz. It is revealed that the difference is related to the changes in southerly wind intensity (integral of southerly wind speed by hours) associated with extratropical cyclones. Third, the interdecadal variability of WH_s is described. The time series of anomalies of WH_s, smoothed by means of a 7-year moving average, is divided into three periods: 1980–1985, 1986–1996, and 1997–2003. The first empirical orthogonal function of 10-m meridional sea surface winds captures the interdecadal variability over the storm track. The smoothed WH_s exhibits similar variation to that of the leading principal component of the winds.

Citation: Sasaki, W., S. I. Iwasaki, T. Matsuura, S. Iizuka, and I. Watabe (2005), Changes in wave climate off Hiratsuka, Japan, as affected by storm activity over the western North Pacific, *J. Geophys. Res.*, *110*, C09008, doi:10.1029/2004JC002730.

1. Introduction

[2] Elucidating the variability of ocean surface waves is of great importance to safe marine transport, offshore industries and the protection of human lives from future coastal disasters. Long-term variability of ocean surface waves is assumed to be related to climate change. The changes in storm activity and global wind patterns may affect the wave conditions, making it necessary to clarify the relationship between the wave variability and climate change.

[3] There are numerous studies on changes in wave climate based on analysis of the observed or hindcast wave data. The NOAA buoy records for the coast of California in the eastern North Pacific show higher waves during major El Niño events and an apparent upward trend over the last 20 years [*Allan and Komar*, 2000]. *Graham and Diaz* [2001] revealed upward trends in winter storm activity and the hindcast wave heights over the North Pacific. The wave heights at the Seven Stones Light Vessels off the SW coast of England show an upward trend [*Carter and Draper*, 1988], and significant wave heights computed from the Comprehensive Ocean–Atmosphere Data Set increase at 10–30 cm/decade over the whole of the North Atlantic, except for the western and central subtropics [*Gulev and Hasse*, 1999]. Numerical wave hindcasts show that increasing trends in significant wave heights at several northeast Atlantic locations since the 1960s are related to systematic deepening of the Icelandic low and intensification of the Azores high over the last three decades [*Kushnir et al.*, 1997]. *Wang and Swail* [2001], applying the empirical orthogonal functions on the global wave hindcast data, report an upward trend in the extreme significant wave heights for the winter mean over the North Atlantic and Pacific since 1960. There are several reports on the analyses of long-term trends in observed significant wave heights around Japan [*Hatada et al.*, 2001, 2002].

[4] Long-term observation of ocean surface waves makes it possible to investigate the relationship between wave variability and climate change; however, long-term monitoring has been carried out only at a few points. The National Research Institute for Earth Science and Disaster Prevention has performed 24-hour continuous wave observation since 1979 at Hiratsuka Marine Observation Tower in Sagami Bay, Japan (Figure 1). The main purpose of this paper is to clarify the cause of the interannual and long-term variability of significant wave heights off Hiratsuka using the observed wave and atmospheric data, and reanalysis data. The interannual and interdecadal variability in the significant wave heights in the western North Pacific have not been fully investigated compared to the wave climate in the North Atlantic.

0148-0227/05/2004JC002730$09.00

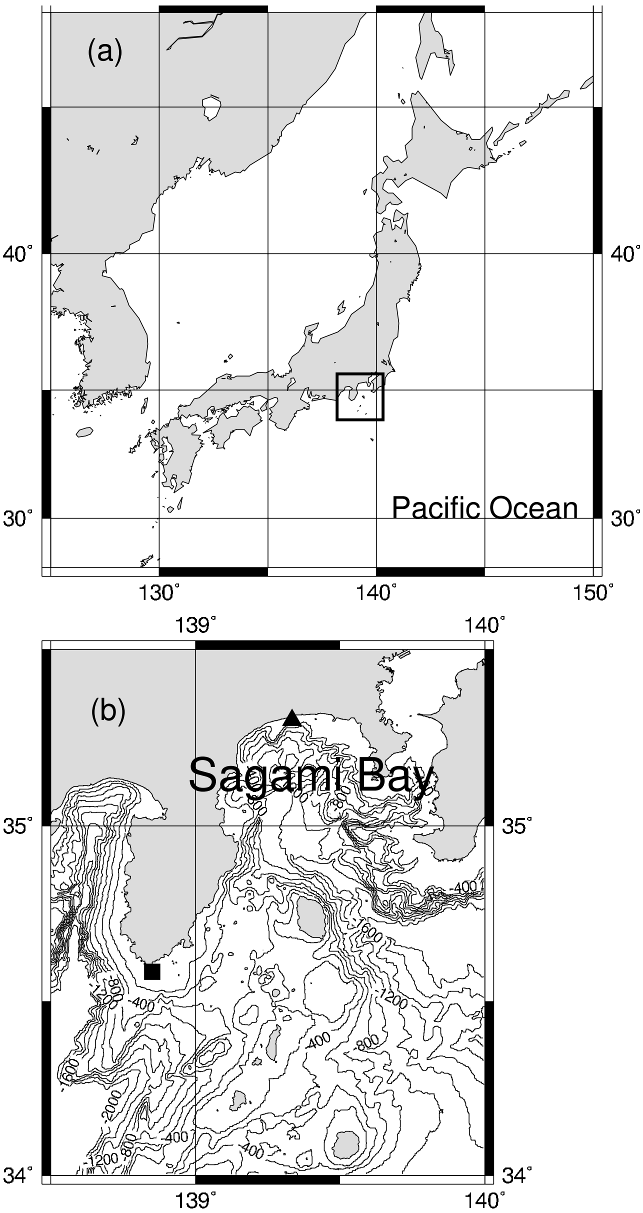

Figure 1. (a) Japan and surroundings. (b) Bathymetric map of the square box shown in Figure 1a. Contour interval is 200 m. The triangle and square mark the observation points off Hiratsuka and Irozaki, respectively.

[5] This paper is arranged in five sections. Section 2 describes the data sets, procedures applied and definition of high and low wave years. Section 3 presents an analysis of the interannual variability of SH_s off Hiratsuka. Section 4 presents the analysis of the interannual and long-term variability of WH_s. Section 5 contains a summary and discussion.

2. Data Description and Definition

2.1. Observed Wave and Atmospheric Data off Hiratsuka and Procedures Applied

[6] 1. Various oceanic and atmospheric variables have been observed at Hiratsuka Marine Observation Tower which is located at the position 139°20′56″E 35°18′07″N, 1 km south from the shore (Figure 1) where the water is 20 m deep. Sea surface elevation is observed by airborne ultrasonic wave gauges. Temperature correction is made using a thermostat and estimated error is less than 1%. Air pressure is observed at 15 m above mean sea level. Wind speed and direction are observed at approximately 23 m above mean sea level. The sea surface elevation, air pressure, and the wind speed and the direction are recorded at 0.3-second intervals continuously for 20 min of every hour.

[7] 2. Significant wave heights are computed by averaging the highest one-third of wave heights from the 20-min sea surface elevation recordings, applying the zero-up-cross method after detrending. Significant wave heights for the summer mean (SH_s) are calculated by averaging the hourly significant wave heights during June–August. Significant wave heights for the winter mean (WH_s) are calculated by averaging the hourly significant wave heights during December–February (e.g., WH_s in 1993 is the significant wave height averaged over the period of December 1992 to February 1993). Figure 2 shows the standardized time series of SH_s and WH_s off Hiratsuka.

[8] 3. Wave energy spectrum ($E(f, t)$ as a function of frequency, f and time, t) is computed every hour using 20 min data (0.3 sec. intervals) by applying spectral analysis (Maximum Entropy Method). The monthly mean $E(f, t)$ is calculated by averaging $E(f, t)$ for each calendar month from 1980 to 2003. $E(f, t)$ for the summer (winter) mean is computed by averaging the monthly $E(f, t)$ from June to August (December to February).

2.2. Significant Wave Heights at Irozaki

[9] To confirm the accuracy of the wave history off Hiratsuka, we also use SH_s at Irozaki, approximately 100 km to the southwest of Hiratsuka. The Japan Meteorological Agency has been conducting the wave measurements since 1976 at 138°51′14″E 34°35′34″N; water depth 50 m (Figure 1b). SH_s at Irozaki is computed by averaging the significant wave heights during June–August. Correlation coefficient between SH_s off Hiratsuka and SH_s at Irozaki is significant at 95% confidence levels ($r = 0.91$).

2.3. Tropical Cyclone Data

[10] In this paper, we use the term tropical cyclone (TC) as a disturbance with maximum sustained wind speed over 17.3 m/s, formed over the western North Pacific. Typhoon best track data during 1980–2003 come from the Regional Specialized Meteorological Center (RSMC) Tokyo Typhoon Center. The data include names, positions (in latitude and longitude), central surface pressure of TCs at intervals of 6 (sometimes 3) hours.

2.4. Reanalysis Data

[11] We use 6-hourly 10 m meridional sea surface wind data based on the NCEP/NCAR reanalysis [*Kalnay et al.*, 1996] during 1980–2003.

2.5. Definition of High and Low Wave Years

[12] Before we define the high and low wave years for summer, a linear trend for the analysis period is removed from the time series of SH_s, and a spectral analysis is applied to the detrended one. SH_s has a spectral peak at 2.6-year cycle (figure is not shown). To analyze the

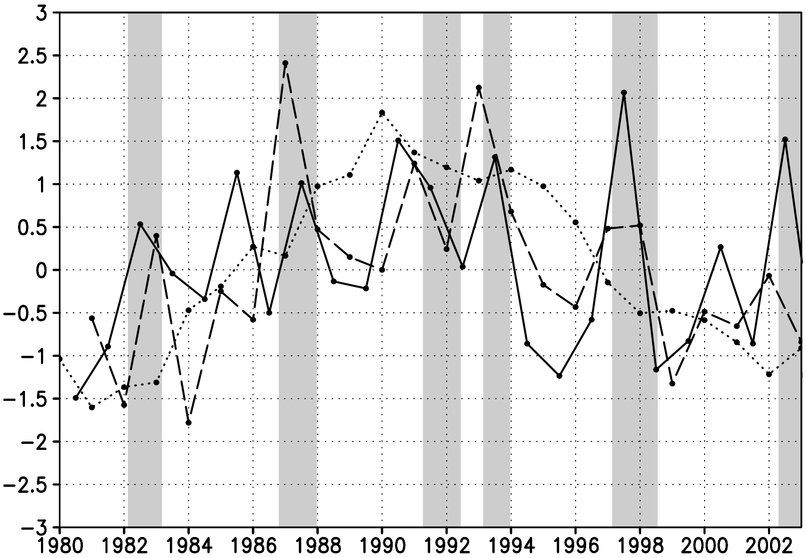

Figure 2. Standardized time series of SH_s (solid line), WH_s (dashed line), and WH_s smoothed by means of a 7-year moving average (dotted line) off Hiratsuka during 1980–2003. Shaded zones indicate El Niño periods.

interannual variability of SH_s, we use the detrended time series of SH_s. The standardization is applied to the time series of SH_s off Hiratsuka and Irozaki, namely, anomalies in SH_s are divided by their standard deviation. High (low) SH_s years are designated when both the standardized values of SH_s off Hiratsuka and Irozaki are greater (less) than 0.5 (−0.5). Both the standardized SH_s are greater than 0.5 in 1982, 1985, 1987, 1990, 1991, 1993, 1997 and 2002 (high SH_s years) and less than −0.5 in 1980, 1981, 1986, 1994, 1995, 1996, 1998, 1999 and 2001 (low SH_s years) (Figure 3).

[13] High and low WH_s years are selected by the same procedures applied to the time series of SH_s. By applying a spectral analysis to the time series of WH_s, it is found that WH_s has two spectral peaks at 4.4- and 22-year cycles. To analyze the interannual variability of WH_s, we use the time series of WH_s excluding means of a 7-year moving average of WH_s. The time series of WH_s smoothed by means of a 7-year moving average is shown in Figure 2. High (low) WH_s years are designated when the standardized values of WH_s are greater (less) than 0.5 (−0.5). Standardized WH_s in 1983, 1987, 1991, 1993, 1997, 1998 and 2002 (high

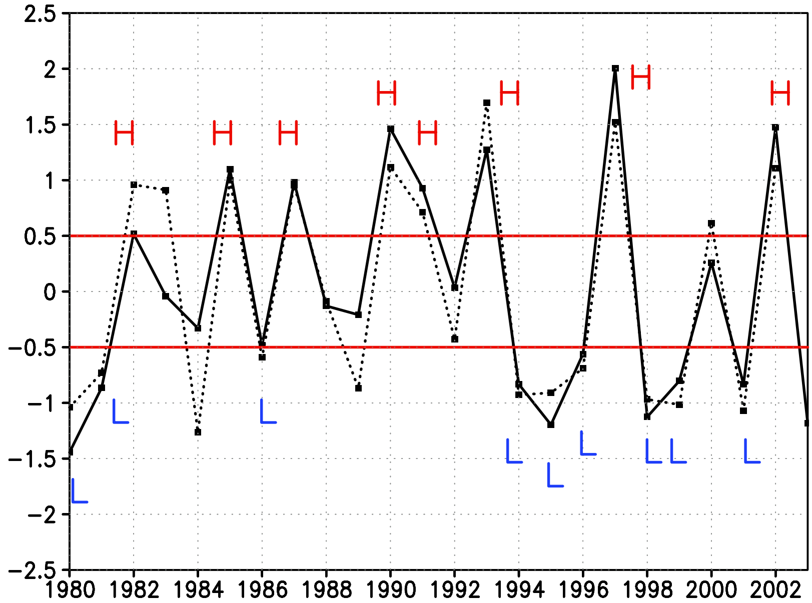

Figure 3. Standardized time series of SH_s off Hiratsuka (solid line) and Irozaki (dotted line) during 1980–2003. High (H) and low (L) SH_s years are defined as values of SH_s over (under) 0.5 (−0.5), respectively. Dimensionless.

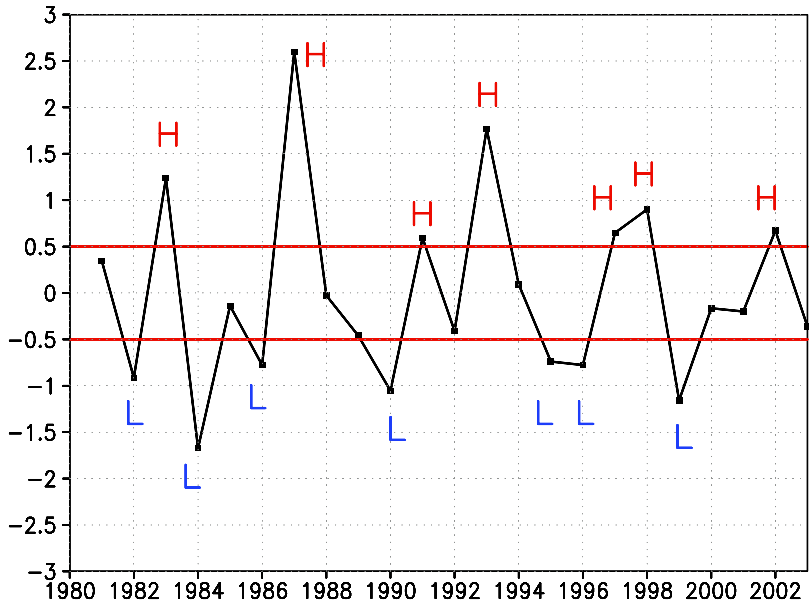

Figure 4. Standardized time series of WH_s off Hiratsuka excluding means of a 7-year moving average. High (H) and low (L) WH_s years are defined as the values of WH_s over (under) 0.5 (−0.5), respectively. Dimensionless.

WH_s years), and less than −0.5 in 1982, 1984, 1986, 1990, 1995, 1996 and 1999 (low WH_s years) (Figure 4).

3. Interannual Variability of SH_s off Hiratsuka

[14] In order to identify the major differences between waves in high SH_s years and those in low SH_s years, we investigate the differences between $E(f, t)$ in high SH_s years and that in low SH_s years. Figure 5 shows averaged $E(f, t)$ for June, July, August and the summer mean in high and low SH_s years. The averaged $E(f, t)$ for June, July, August and the summer mean have higher values across all frequencies in high SH_s years than in low SH_s years. In particular, the largest difference in the averaged $E(f, t)$ for

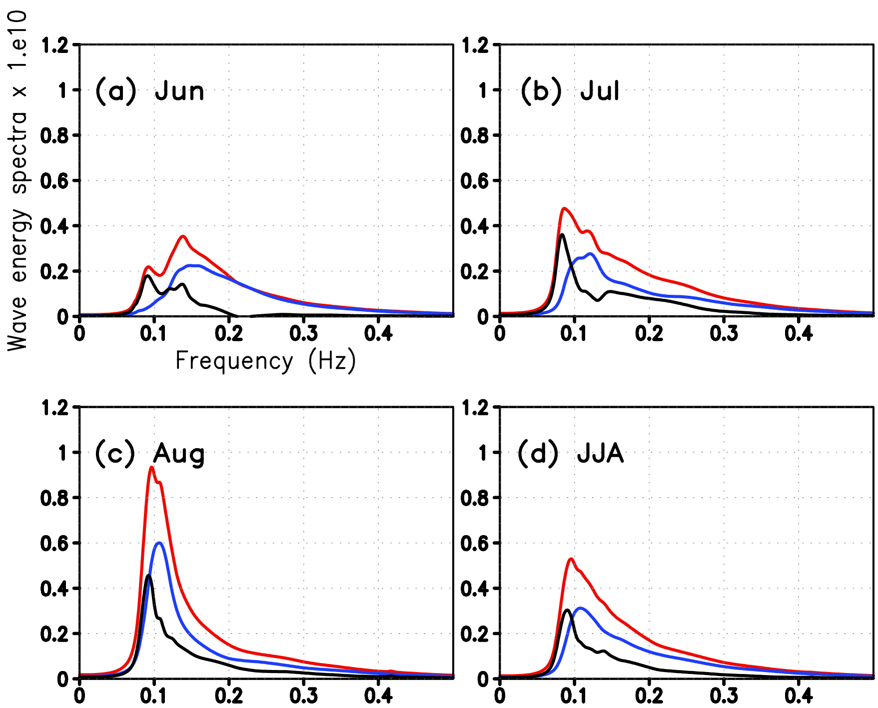

Figure 5. $E(f, t)$ (cm^2 s) off Hiratsuka in (a) June, (b) July, (c) August, and (d) the summer mean. Red and blue lines show the averaged wave spectrum for high and low SH_s years, respectively. Black line indicates the difference between $E(f, t)$ for the summer mean in high SH_s years and that in low SH_s years.

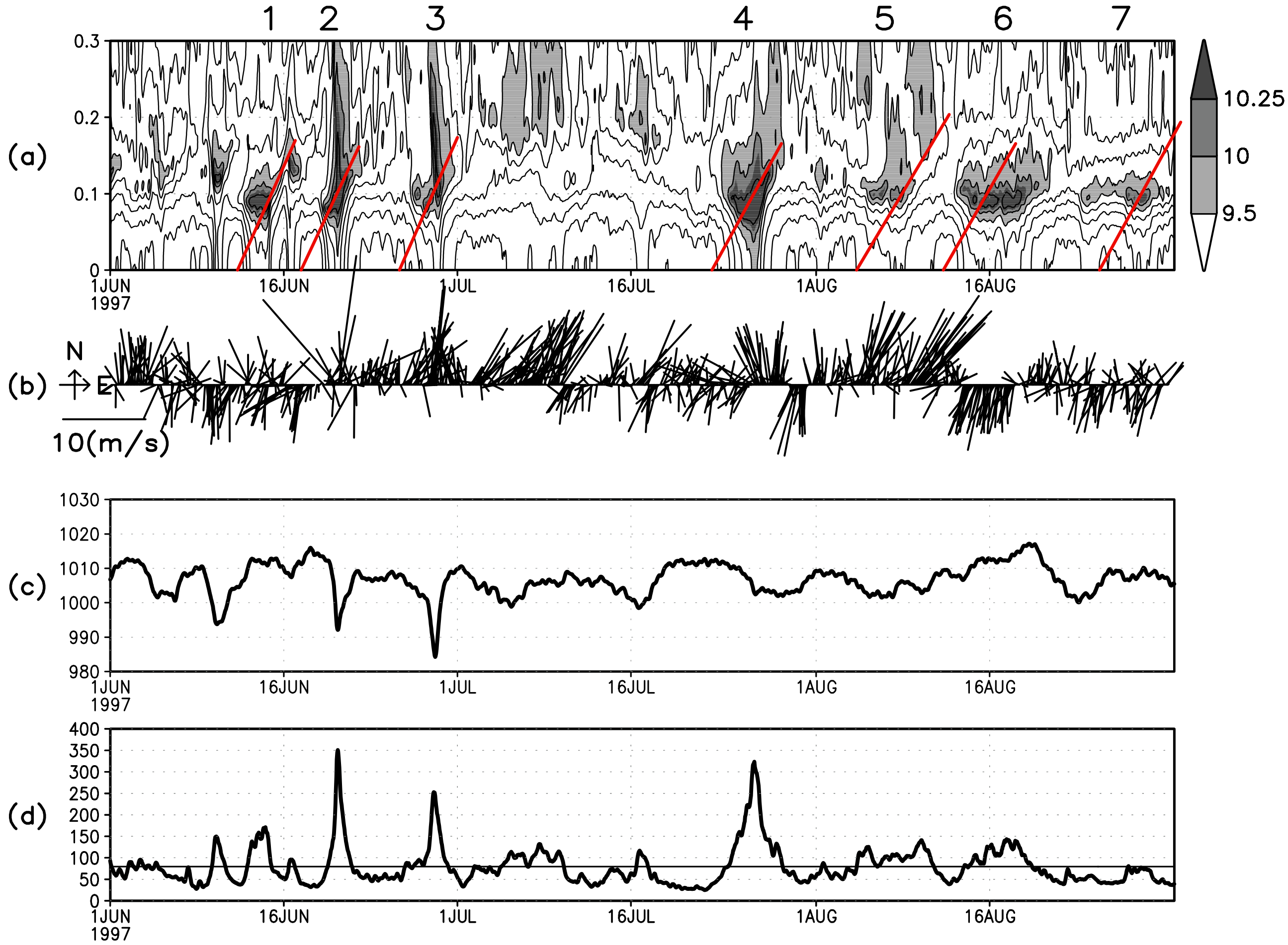

Figure 6. (a) Time series of $\log_{10}E(f, t)$ (cm^2 s), (b) stick diagram of wind vectors, (c) air pressure (hPa), and (d) significant wave heights (cm) off Hiratsuka during 1 June 1997, 0000 UTC to 31 August, 2300 UTC. The time series of $\log_{10}E(f, t)$, air pressure, and significant wave heights are smoothed by means of a 6-hour moving average. Contour interval in Figure 6a is 0.5, and the shaded region indicates where $\log_{10}E(f, t)$ exceeds 9.5. The vertical axis of Figure 6a indicates the frequency (Hz). There are seven events where the peak frequency is strong below 0.1 Hz. Corresponding numbers are shown at the top of Figure 6a. Line in Figure 6a marks the ridgeline drawn by using a 6-hour linear interpolation from the minimum peak frequency. The stick diagram of wind vectors in Figure 6b is drawn at 3-hour intervals. The horizontal line in Figure 6d exhibits significant wave heights for the summer mean in 1997.

the summer mean is observed at the frequency of 0.09 Hz (Figure 5d). This result implies that the frequency and strength of swells whose period is 11.1 s contribute more to the increase in significant wave heights in high SH_s years than in low SH_s years. We investigate the time series of $E(f, t)$ and significant wave heights, and the atmospheric condition at the tower in detail by taking 1997 as an example.

[15] Figure 6a shows the time series of $\log_{10}E(f, t)$ off Hiratsuka during 00Z01 June 1997 to 23Z31 August 1997. We focus on the low frequency waves whose frequency is below 0.1 Hz, since the largest difference between the averaged $E(f, t)$ for the summer mean in high SH_s years and that in low SH_s years is found at the frequency of 0.09 Hz. We now introduce the criteria for selecting events where there is a sharp peak below 0.1 Hz and where $\log_{10}E(f, t)$ is larger than 10.0. There were seven notable events which met the criteria during June–August 1997 (the numbers are shown above Figure 6a). Most of the increase in significant wave heights corresponds to the selected events. In June 1997, there were three events as shown in Figure 6. Compared with the time series of $\log_{10} E(f, t)$ and that of significant wave heights in June 1997, significant wave heights began to increase when a sharp spectral peak emerged at low frequencies and increased dramatically when the sharp spectral peak shifted to high frequencies (events 2 and 3 in Figure 6a). Therefore these spectral peaks at low frequencies could be identified as presaging an increase in significant wave heights. The shift of spectral peak to high frequencies occurred when the wind speed increased and the air pressure dropped suddenly (Figures 6a–6c). These results imply that the significant wave heights off Hiratsuka began to increase starting with swells of which the period is initially around 10 s, and increased as a result of the swells and wind waves caused by the passage of disturbance. Therefore a spectral peak at low

Table 1. List of TC Numbers for Seven Events As Shown at the Top of Figure 6a, Corresponding to t_0 and Δ Computed by Frequency-Time Plot[a]

Number	TC Number	t_0 Date	Δ, km	Latitude, deg	Pressure, hPa
1	T9706	12z11 June 1997	2034	20.6	935
2	T9707	00z17 June 1997	2194	16.4	975
3	T9708	12z25 June 1997	2272	18.8	990
4	T9709	12z22 July 1997	2519	18.2	935
5	T9711	00z04 August 1997	2520	17.1	970
6	T9713	12z11 August 1997	2552	16.6	950
7	T9716	00z25 August 1997	2977	17.5	955

[a]The pressure and latitude, obtained by typhoon best track data, show the central pressure of the TC and the TC's latitudinal position at the time of t_0, respectively.

frequencies can be regarded as a predictor of increased significant wave heights off Hiratsuka.

[16] There were four events in July and August 1997 (events 4–7 in Figure 6a). In the three events (events 4–6), significant wave heights increased to more than the mean value despite the wind speed and air pressure not changing drastically. These results support the conclusion that propagating swells contribute enormously to the increase in the significant wave heights off Hiratsuka.

[17] To detect the wave sources of the swells, a frequency-time plot [*Snodgrass et al.*, 1966] is applied to $E(f, t)$ during June–August 1997.

[18] As *Snodgrass et al.* [1966] showed, let Δ be the distance from a source to the tower, t_0 the time of wave generation, and t the time of recording. We regard the propagating waves as deep-water waves. Although the water depth is 20 m at the tower, the water depth at several kilometers south of the tower increases to over 400 m in Sagami Bay (Figure 1b). The group velocity in deep water, $V(f)$ is written as follows.

$$V(f) = \frac{\Delta}{t - t_0} \tag{1}$$

In deep water,

$$V(f) = \frac{g}{4\pi f}. \tag{2}$$

It follows that

$$f = \frac{g}{4\pi\Delta}(t - t_0). \tag{3}$$

Therefore on a plot of f against t, a single event lies along a straight line with slope

$$\frac{df}{dt} = \frac{g}{4\pi\Delta} \tag{4}$$

and intercept $f = 0$, at $t = t_0$. Each ridgeline can be immediately associated with a wave source of known distance and time. The hourly spectral peak is computed using $\partial E(f, t)/\partial f = 0$. The slope of the ridgeline (df/dt) is estimated by a linear interpolation of spectral peaks of 12 hours from the peak with the lowest frequency. Δ and t_0 are computed from equations (3) and (4) for each event (Table 1).

[19] The red lines in Figure 6a are the ridgelines for the selected seven events in summer in 1997. Mean Δ is estimated at approximately 2400 km. This result suggests that tropical cyclones (TCs) formed in the western North Pacific are a possible wave source. TC's latitudinal position and the central pressure corresponding to the time t_0 are obtained from the typhoon best track data (Table 1). A check of t_0, Δ and TC tracks in typhoon best track data suggests that each wave source is generated by an enhanced TC, defined as a TC whose central pressure is below 980 hPa, locates within 2400 km of the tower in the western North Pacific (Table 1, Figure 7). Figure 7, numbers 1–7 exhibit the tracks of seven TCs which correspond to the seven events at the tower. The central pressure of the TCs began to fall below 980 hPa when the TCs passed across approximately the 20°N line. Swells formed by these enhanced TCs propagate to the tower and are observed as the predictor of an increase in significant wave heights even if their tracks are far from the tower. On the other hand, swells generated by weak TCs do not cause any apparent increase in significant wave heights. Figure 7 (number 8) shows TC tracks in summer 1997 except those of the seven TCs shown in Figure 7 (numbers 1–7). These TCs are relatively weak (central pressure is over 980 hPa) and their tracks are far from the tower. We therefore conclude that the swells caused by the enhanced TCs that locate within 2400 km of the tower in the western North Pacific contribute to the increases in significant wave heights off Hiratsuka.

[20] This result suggests that the interannual variability of SH_s off Hiratsuka corresponds to the variability of enhanced TC passage frequency over the western North Pacific. Figure 8 shows a comparison between the TC tracks in both high SH_s years and in low SH_s years. The enhanced TC passage frequency in June, July and August in high SH_s years are more common than those in low SH_s years. In particular, the enhanced TCs pass over the western North Pacific more frequently in August in high SH_s years than in low SH_s years. This result coincides with the large difference in the shape of the spectral peak in August between in high and low SH_s years (Figure 5c).

[21] As shown in Figure 2, SH_s increases during El Niño summers. Our results therefore indicate a relationship between TC enhancement, track and the El Niño effect over the western North Pacific in summer. We discuss this relationship in Section 5.

4. Interannual and Long-Term Variability of WH_s off Hiratsuka

[22] In this section, the interannual and interdecadal variability in WH_s off Hiratsuka are described. In Section 4.1, we analyze the cause of the interannual variability of WH_s. In Section 4.2, we investigate the relationship between the interdecadal variability of WH_s and the storm track activity over the western North Pacific. In this paper the term "storm track" signifies a long-term average of cyclone paths. The path of the cyclones shows good agreement with the winter storm track [*Whitaker and Horn*, 1984].

4.1. Interannual Variability of WH_s off Hiratsuka

[23] To identify the differences between waves in high WH_s years and those in low WH_s years, $E(f, t)$ in high WH_s

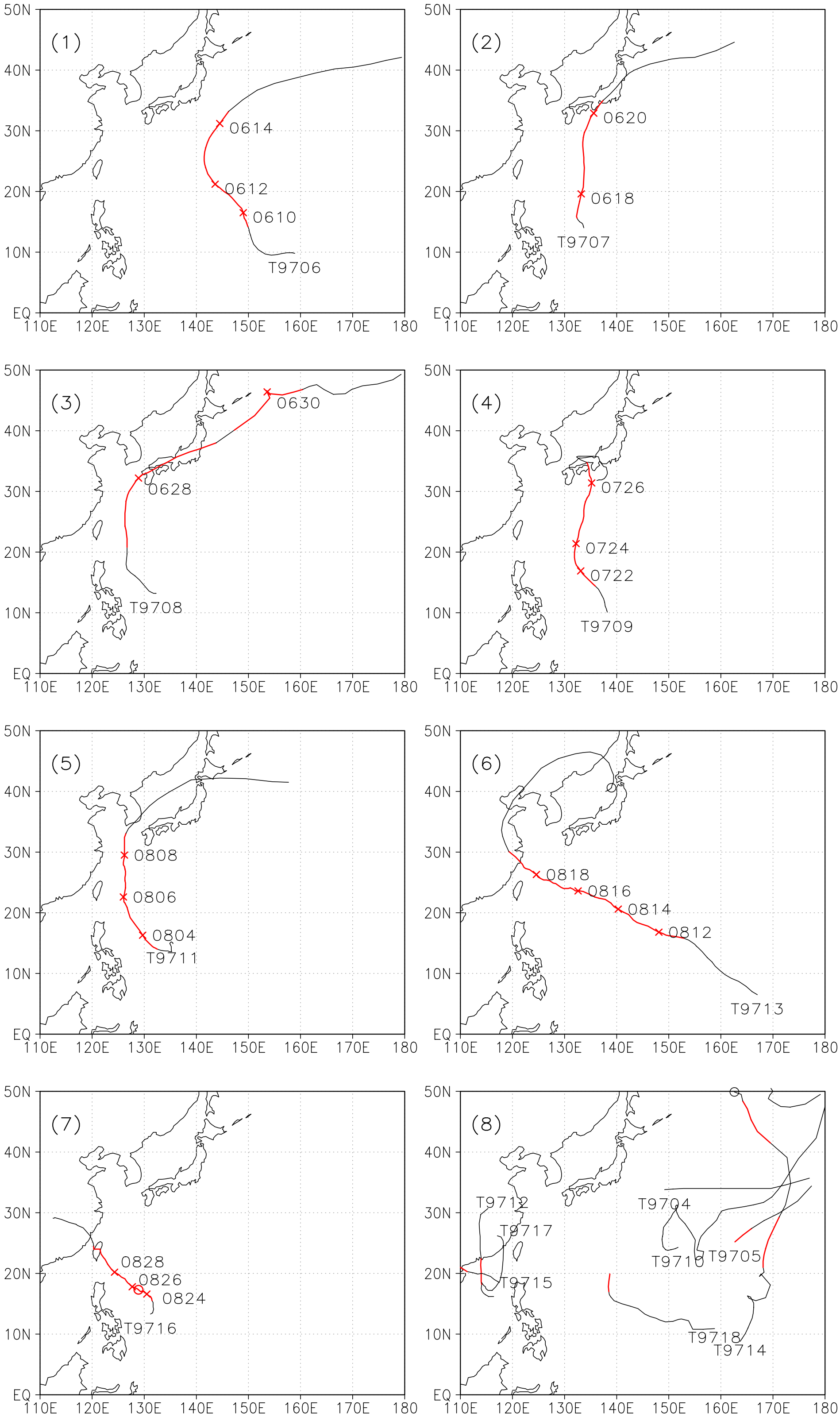

Figure 7. In this figure, numbers 1–7 show the tracks of TCs that generated swells with peak frequency below 0.1 Hz at the tower during June–August 1997. They also correspond to the numbers on the top of Figure 6a. Red shows the tracks of TCs whose central pressure was below 980 hPa. The number beside the track shows the date when the TC was located at the position shown by the cross (e.g., number 610 means 10 June, 0000 LT). The circle shows the position of TC at time t_0 (Table 1). The index on the bottom of the track gives the TC number. Number 8 exhibits the tracks of eight other TCs (TC numbers T9704, T9705, T9710, T9712, T9714, T9715, T9717, and T9718 are shown) during June–August 1997.

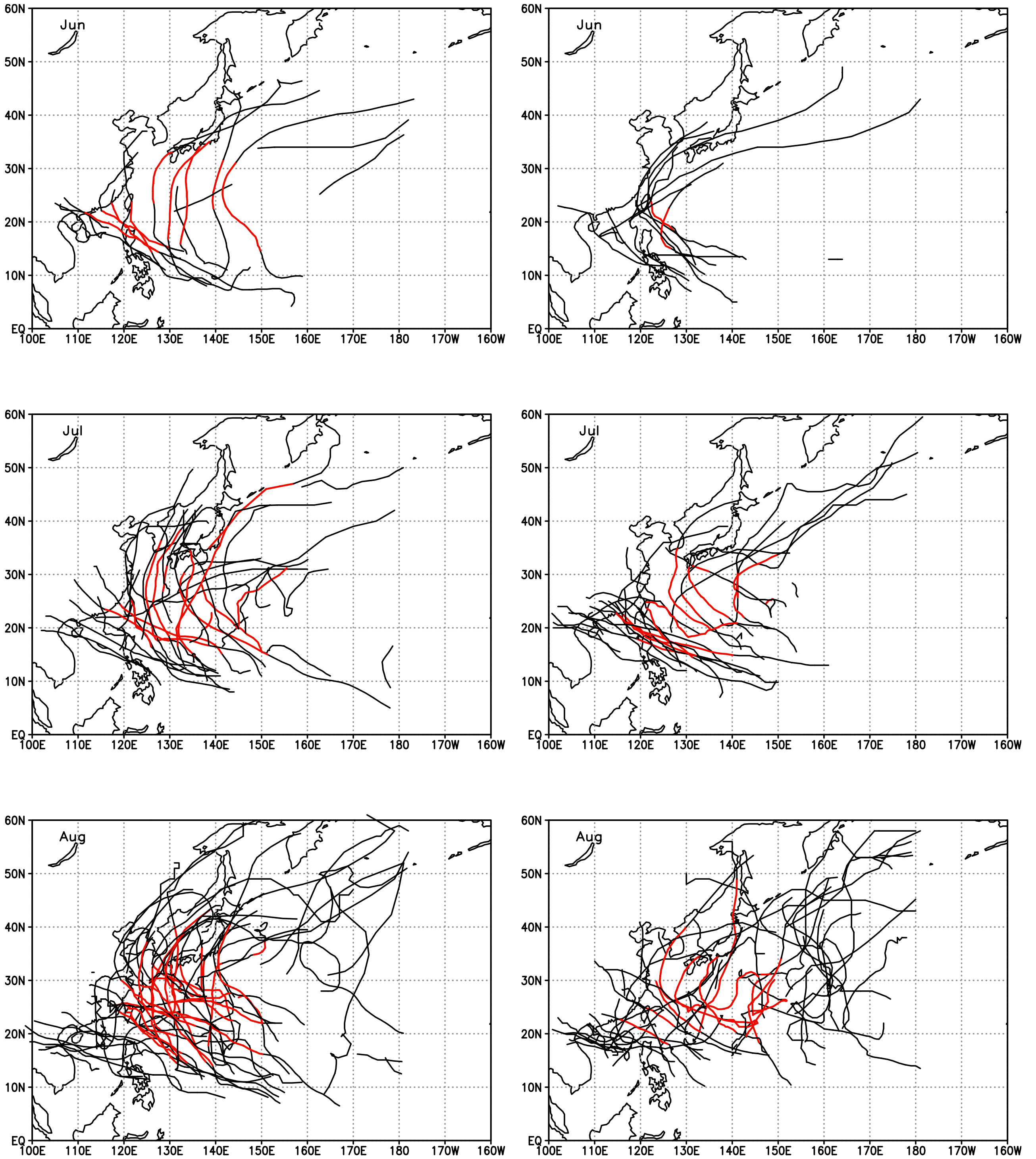

Figure 8. Comparison of TC tracks between the highest eight SH_s years (left panels) and the lowest eight SH_s years (right panels) in June, July, and August. The top, middle, and bottom plots show TC tracks in June, July, and August, respectively. Red shows TC tracks whose central pressure is below 980 hPa.

years and that in low WH_s years are contrasted. Figure 9 shows averaged $E(f, t)$ for December, January, February and the winter mean in high and low WH_s years. The averaged $E(f, t)$ has higher values across all frequencies in high WH_s years than in low WH_s years. In particular, the largest difference in averaged $E(f, t)$ for the winter mean is observed at the frequency of 0.11 Hz (Figure 9d). This result implies that waves whose period is 9.1 s contribute more to the increase in significant wave heights in high WH_s years than in low WH_s years. The difference in waves at the frequency of 0.11 Hz may be due to wind waves. We investigate the relationship between the variation in significant wave height and the atmospheric conditions at the tower in detail by taking 1993 as an example.

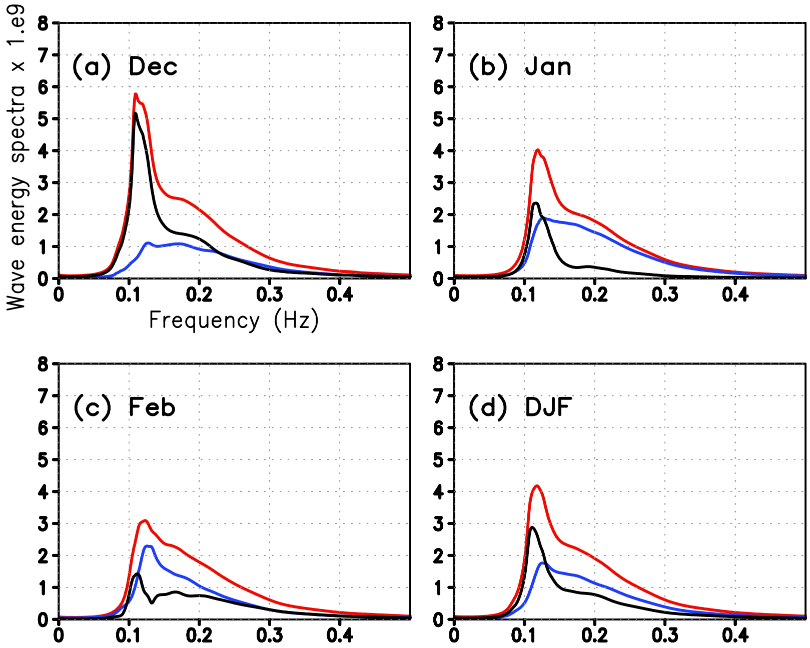

Figure 9. $E(f, t)$ (cm^2 s) off Hiratsuka in (a) December, (b) January, (c) February, and (d) winter mean. Red and blue lines indicate the mean spectrum for high and low WH_s years, respectively. Black line indicates the difference between averaged $E(f, t)$ for the winter mean in high WH_s years and that in low WH_s years.

[24] Figure 10 shows the time series of $\log_{10} E(f, t)$, wind stick diagram, air pressure and significant wave heights at the tower during 00Z01 December 1992 to 23Z28 February 1993. The increases in significant wave heights correspond to strong peaks of $E(f, t)$ at over 0.1 Hz (Figures 10a and 10d). Significant wave heights appear to increase when the air pressure drops and southerly winds intensify (Figures 10b–10d). Correlation coefficient between significant wave heights and air pressure during the period is −0.60. This result suggests that the increase in significant wave heights at the tower is associated with passages of disturbance. We now refer to the relationship between the increase in significant wave heights and wind direction at the tower. Figure 11 shows the rate of high wave (significant wave heights over 1 m) occurrence on the wind direction during 00Z01 December 1992 to 23Z28 February 1993. The high waves occur when southwesterly and northerly winds blow. Although the northerly winds have higher occurrence than the southwesterly winds at the tower (Table 2), the southerly winds impact on the increase in significant wave heights. This is explained by the alignment of Sagami Bay. Since Sagami Bay opens to the south (Figure 1b), the waves grow with the long fetch length and time, propelled by southerly winds. The fetch length by northerly winds is short, since the tower is located 1 km south of the shore. The strength of southerly wind plays an important role on the interannual variability of WH_s. The difference in southerly wind speed between in high WH_s years (1987 and 1993) and in low WH_s years (1990 and 1999) is remarkable, however there is no apparent difference in northerly wind speed between in high WH_s years and in low WH_s years (Figure 12). We therefore conclude that the interannual variability of WH_s off Hiratsuka is due to the interannual variability of the strength of southerly winds.

[25] To confirm the relationship between the interannual variability of WH_s and that of southerly winds, we demonstrate the comparison of the time series of WH_s and that of southerly wind intensity over the southern part of Japan by using reanalysis wind speed. The southerly wind intensity is designated as the hourly integral of the southerly wind speed. To estimate the southerly wind intensity, 6-hourly meridional sea surface wind speed of NCEP-NCAR reanalysis is employed. The time series of WH_s and the southerly wind intensity averaged over the region of 30°N–40°N, 130°E–150°E are shown in Figure 13. Their correlation coefficient is 0.71. We conclude that the interannual variability of WH_s off Hiratsuka results from the interannual variability of the southerly wind intensity over the south of Japan.

[26] As shown in Figure 10b, monsoonal flow over Japan in winter is characterized by northerly winds associated with the Siberian high and the Aleutian low. Although the northerly winds have higher occurrence than the southerly winds (Table 2), mean southerly wind speed is larger than that of northerly winds (Figure 12). The incidence of the southerly winds associated with a drop in air pressure (Figures 10b and 10c) suggests the passage of winter cyclone. These cyclones are generated over the East China Sea and pass along the south of Japan [*Hanson and Long*, 1985]. *Hanson and Long* [1985] documented that extratropical cyclones occur more frequently over the East China Sea in El Niño years than in normal years. WH_s off Hiratsuka also increase in the El Niño winters of 1983, 1987, 1993, 1997, 1998 and 2002.

4.2. Interdecadal Variability of WH_s off Hiratsuka

[27] The time series of WH_s smoothed by means of a 7-year moving average is divided into 3 regimes: 1980–

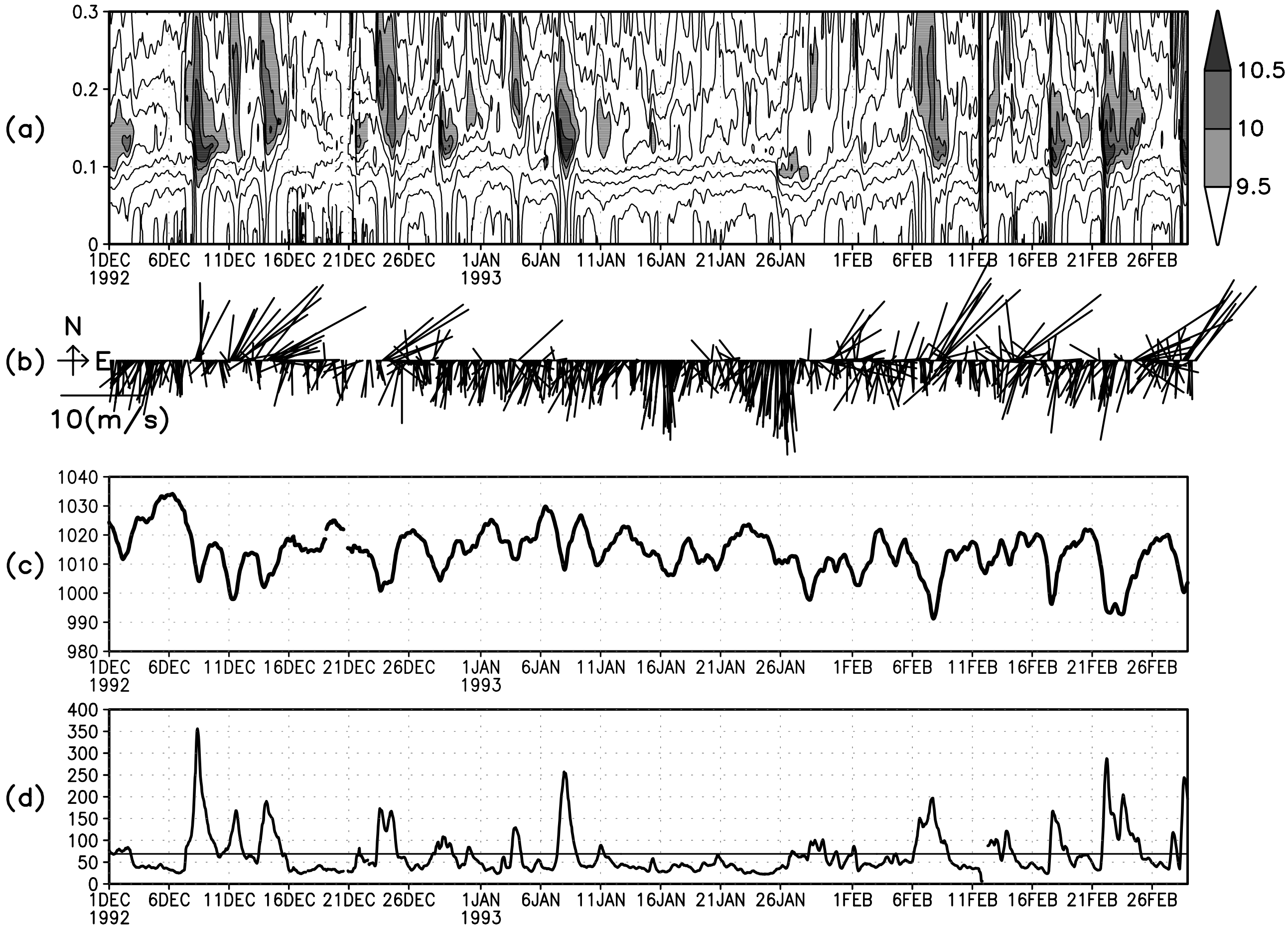

Figure 10. (a) Time series of $\log_{10}E(f, t)$ (cm^2 s), (b) stick diagram of wind vectors, (c) air pressure (hPa), and (d) significant wave heights (cm) during 1 December 1992, 0000 UTC to 28 February 28 1993, 2300 UTC. The time series of $\log_{10}E(f, t)$, air pressure, and significant wave heights are smoothed by means of a 6-hour moving average. Contour interval in Figure 10a is 0.5, and the shaded region indicates where $\log_{10}E(f, t)$ exceeds 9.5. The wind stick diagram in Figure 10b is drawn at 3-hour intervals. The horizontal line in Figure 10d illustrates the significant wave heights for the winter mean in 1993.

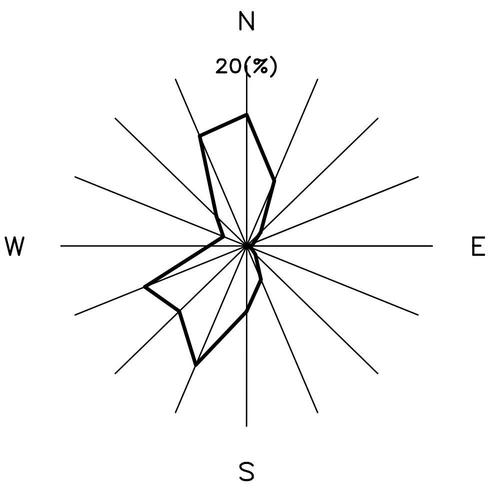

Figure 11. Percentage of high wave (significant wave heights over 1 m) occurrence on wind directions at the tower during 00Z01 December 199 to 23Z28 February 1993.

Table 2. Percentage of Wind Direction off Hiratsuka in High and Low WH_s years[a]

Wind Direction, %	High WH_s Years 1987	High WH_s Years 1993	Low WH_s Years 1990	Low WH_s Years 1999
N	**34.3**	**34.9**	**43.2**	**36.7**
NNE	**22.7**	**19.3**	**20.5**	**11.2**
NE	6.7	7.1	5.2	3.1
NEE	2.5	2.7	1.5	1.9
E	0.9	0.9	0.7	0.8
SEE	1.5	1.3	1.4	1.6
SE	1.7	1.7	1.3	2.0
SSE	2.2	1.9	1.6	3.2
S	2.5	3.1	2.6	4.1
SSW	4.2	3.7	3.4	2.6
SW	5.9	4.4	4.3	3.5
SWW	3.2	2.8	1.7	3.5
W	2.7	3.9	1.6	2.0
NWW	1.0	1.9	0.8	1.5
NW	0.9	1.7	1.8	2.8
NNW	6.7	8.3	8.2	**18.7**

[a]Boldface indicates percentages exceeding 10%.

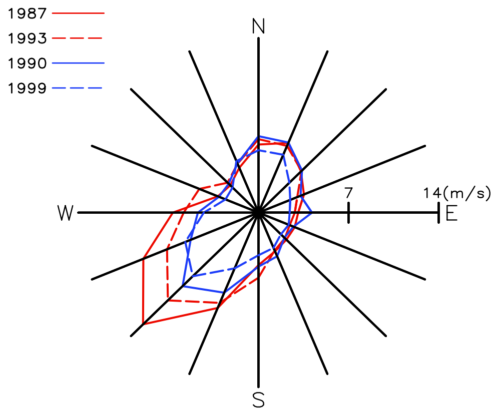

Figure 12. Wind velocity (m/s) for the winter mean off Hiratsuka in 1987 (red solid line), 1993 (red dotted line), 1990 (blue solid line), and 1999 (blue dotted line). Red and blue lines show the high and low WH_s years, respectively.

1985, 1986–1996 and 1997–2003 (Figure 2 (dotted line)). As described in the previous subsection, the increase in WH_s is caused by the increase in southerly wind intensity over the southern part of Japan. Therefore it is supposed that the variability of WH_s is related to the variability of meridional wind speed. We applied an empirical orthogonal function (EOF) analysis to the 10 m sea surface meridional winds (V_{10m}) for the winter mean over the western North Pacific (100°E–180°E, 20°N–50°N) during 1980–2003. The EOF analysis was conducted after the wind data was detrended and smoothed by means of a 7-year moving average to remove the relatively high-frequency variability. The map (Figure 14a) of the coefficient of linear regression between V_{10m} and the leading principal component (PC1) of V_{10m} exhibits intensification of V_{10m} over the path of winter cyclone in the western North Pacific. The time series of PC1 of V_{10m} shows variability similar to the time series of WH_s smoothed by means of a 7-year moving average (Figure 14b). This result indicates that the interdecadal variability of WH_s corresponds to the variation in storm track activity over the western North Pacific. As *Nakamura et al.* [2002] documented, the storm track activity over the western North Pacific has the decadal modulation and increased in the late 1980s. Our results clarify the correspondence between the interdecadal variability of the activity in the extratropical cyclone and the changes in wave climate over the southern coast of Japan in winter.

5. Summary and Discussion

[28] Changes in wave climate off Hiratsuka since 1980 have been analyzed based on the hourly observed wave and atmospheric data, and reanalysis data.

5.1. Summer

[29] We have described that the interannual variability of SH_s off Hiratsuka is due to changes in enhanced tropical cyclone (TC) activity over the western North Pacific. This result was obtained by the three steps of our analysis: (1) A marked difference between wave energy spectrum ($E(f, t)$) in high SH_s years and that in low SH_s years was found at the frequency of 0.09 Hz. This result indicates that swells contribute more to waves in high SH_s years than in low SH_s years. (2) It was found, by computing the time of wave generation t_0 and the distance from a wave source to the tower Δ, and tracing the typhoon best track data of summer 1997, that the swells are formed by enhanced TCs which locates within 2400 km of the tower in the western North Pacific. (3) The enhanced TC passage frequency over the western North Pacific is higher in high SH_s years than in low SH_s years.

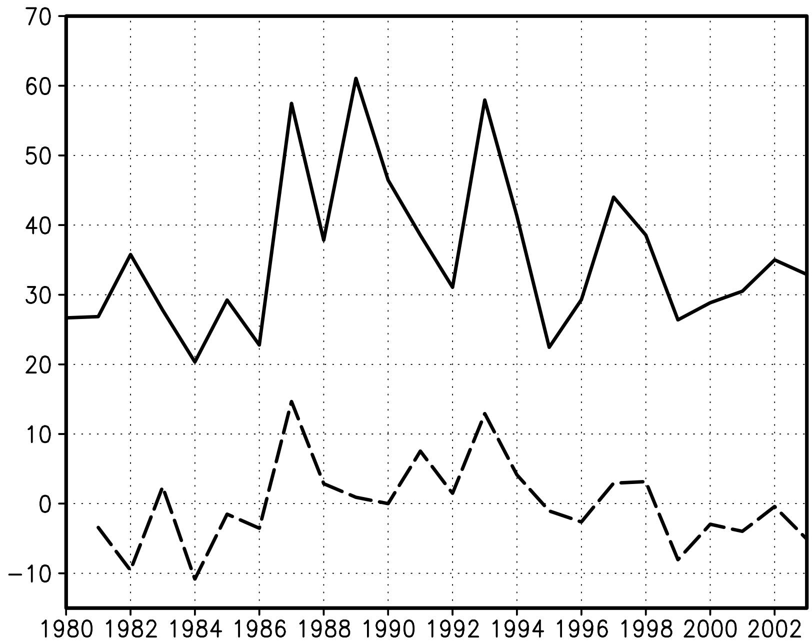

Figure 13. Time series of southerly wind intensity (m/s × day) averaged over the region of 130E–150E, 30N–40N (solid line), and anomalies of WH_s (cm) off Hiratsuka (dotted line).

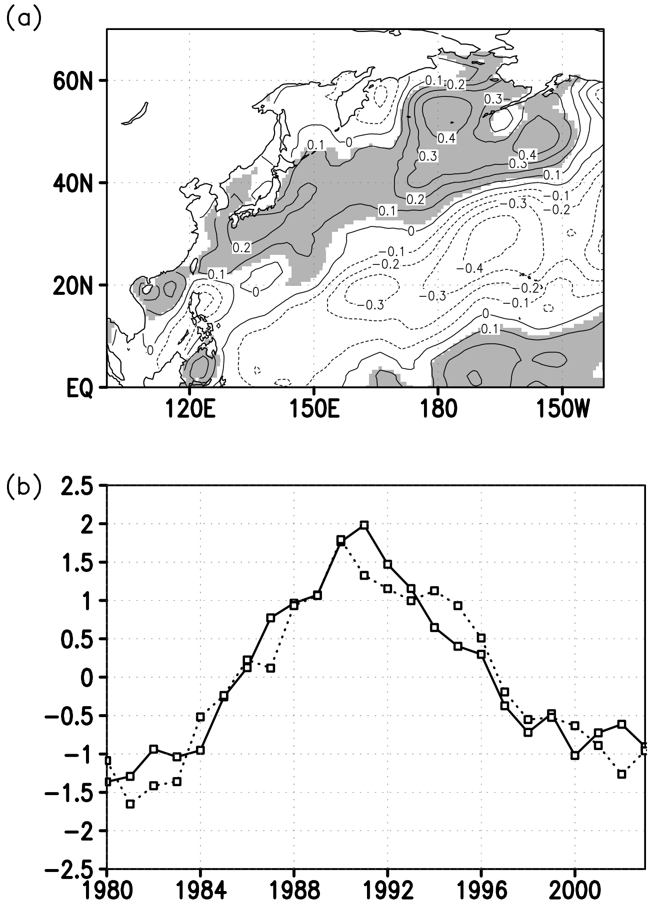

Figure 14. (a) Map of the coefficient of linear regression between V_{10m} and the leading principal component (PC1) of V_{10m}. The shaded regions indicate where the local correlation with PC1 exceeds the 95% confidence level. (b) Time series of PC1 of V_{10m} (solid line) and WH_s smoothed by means of a 7-year moving average (dotted line).

[30] We now refer to the relation between the TC tracks and enhancement and El Niño event, since SH_s have positive anomaly during El Niño summers (Figure 2). Table 3 shows the frequency of TCs which took westward tracks across 120°E line among TCs which occurred in the region of 0°–35°N, 120°–160°E in high and low SH_s years. In low SH_s years, 47% of TCs took westward track across the 120°E line, whereas 34% of TCs took westward tracks across the 120°E line in high SH_s years. Fewer TCs take westward track across 120°E line in high SH_s years than in low SH_s years. The higher number of TCs which take northward track may affect the increase in SH_s. *Wang and Chan* [2002] documented that there is an apparent difference in TC tracks during September–November (SON) between strong El Niño and La Niña years. They revealed that TCs tend to recurve northward to the extratropics during SON in strong El Niño years, whereas during strong La Niña years, TCs more frequently take westward tracks. Our analysis suggests that there might also be changes in the TC tracks during June–August between El Niño and La Niña years.

[31] TC enhancement as well as their tracks play important roles in the increase in SH_s. In the highest eight SH_s years, 70% of TCs whose central pressure fell below 980 hPa (there are 61 enhanced TCs among 94 formed TCs). In contrast, 46% of TCs whose central pressure fell below 980 hPa (there are 45 enhanced TCs among 84 formed TCs) were in the lowest eight SH_s years. TC enhancement rather than their genesis frequency plays an important role on the interannual variability of SH_s, since swells formed by weak TCs far from Japan might not propagate as far as Hiratsuka. In fact, the interannual variability of SH_s is not correlated with the number of TCs generated in the western North Pacific: their correlation coefficient is 0.22.

[32] Considering a large difference between the number of enhanced TCs in high SH_s years and that in low SH_s years in the western North Pacific (Figure 8), wave heights in the western North Pacific as well as around the southern coast of Japan may have an interannual variability similar to that off Hiratsuka. Further observed wave data recorded at various stations, and numerical hindcasting, are needed to understand the changes in wave climate over the western North Pacific.

5.2. Winter

[33] We have clarified that the interannual variability of WH_s off Hiratsuka is affected by the changes in winter cyclone activity over the storm track. In particular, the interannual variability of WH_s corresponds to that of southerly wind intensity (hourly integral of southerly wind speed) over the south of Japan. This result was obtained from the three steps of our analysis: (1) A marked difference between averaged $E(f, t)$ for the winter mean in high WH_s years and that in low WH_s years was found at the frequency of 0.11 Hz. This result indicates that wind waves contribute more to the waves in high WH_s years than in low WH_s years. (2) It was revealed that the wind waves are caused by passage of disturbance by investigating the time series of significant wave heights, air pressure and wind direction at the tower in winter in 1993. In particular, southwesterly winds associated with the disturbance increase WH_s with respect to the interannual variability. (3) It was found, by using reanalysis wind data, that the interannual variability of WH_s is explained by the variability of southerly wind intensity over the southern part of Japan. Correlation between WH_s and the southerly wind intensity is significant at 95% confidence

Table 3. The Number of TCs That Took Westward Track Across 120°E Line in High and Low SH_s Years[a]

High SH_s Years	Across	Not Across	Low SH_s Years	Across	Not Across
1982	4	6	1980	5	2
1985	2	8	1981	4	8
1987	2	7	1986	2	6
1990	4	7	1994	8	4
1991	6	4	1995	4	2
1993	4	7	1996	3	5
1997	2	7	1998	2	1
2002	3	6	1999	2	5
			2001	4	5
Total	34%	66%		47%	53%

[a]"Across" indicates the number of TCs that took westward track across 120°E line. "Not across" indicates the number of TCs that did not take westward track across 120°E line. The percentages of the number of TCs among the total number of TCs is recorded on the last line.

level (r = 0.71). The southerly winds are caused by winter cyclones that pass along the south of the Japan. Higher cyclone occurrence over the East China Sea in El Niño winters than in normal winters [*Hanson and Long*, 1985] may contribute to the increase in WH_s off Hiratsuka.

[34] We have investigated the interdecadal variability of WH_s off Hiratsuka. The time series of WH_s, smoothed with a 7-year moving average, shows the interdecadal variability. The smoothed time series is divided into three regimes: 1980–1985, 1986–1996 and 1997–2003. EOF analysis was applied to V_{10m} over the western North Pacific during 1980–2003 after the data is smoothed by means of a 7-year moving average. The map (Figure 14a) of the coefficient of linear regression between V_{10m} and the leading principal component (PC1) of V_{10m} shows significant intensification of V_{10m} over the paths of winter cyclones. The three regimes in WH_s show good agreement with the variability of the PC1 (Figure 14b). These results indicate that storm track activity affects the changes in wave climate off Hiratsuka with respect to the interdecadal variability.

[35] Although 4.4- and 22-year cycles are captured by applying spectral analysis to the time series of WH_s, the length of the time series of WH_s is not sufficiently long to confirm the peak periods. Longer-period observed wave data are needed to confirm the interdecadal variability.

References

Allan, J. C., and P. D. Komar (2000), Are ocean wave heights increasing in the eastern North Pacific?, *Eos Trans. AGU*, *47*, 561–567.

Carter, D. J. T., and L. Draper (1988), Has the northeast Atlantic become rougher?, *Nature*, *332*, 494.

Graham, N. E., and H. F. Diaz (2001), Evidence for intensification of North Pacific winter cyclones since 1948, *Bull. Am. Meteorol. Soc.*, *82*(9), 1869–1893.

Gulev, S. K., and L. Hasse (1999), Changes of wind waves in the North Atlantic over the last 30 years, *Int. J. Climatol.*, *19*, 1091–1117.

Hanson, H. P., and B. Long (1985), Climatology of cyclogenesis over the East China Sea, *Mon. Weather Rev.*, *113*, 697–707.

Hatada, Y., M. Yamaguchi, M. Ohfuku, M. J. Li, and H. Nonaka (2001), Applicability of a 20-year wave hindcast system to the wave estimation on coastal area of Japan (in Japanese), *J. Jpn. Soc. Nat. Disaster Sci.*, *20-3*, 307–324.

Hatada, Y., M. Yamaguchi, M. Ohfuku, M. J. Li, and H. Nonaka (2002), Estimation of long term variability of wave height climate around the coastal sea areas of Japan (in Japanese), *Ann. J. Eng. Ehime Univ.*, *1*, 217–229.

Kalnay, E., et al. (1996), The NCEP/NCAR 40-yr reanalysis project, *Bull. Am. Meteorol. Soc.*, *77*, 437–471.

Kushnir, Y., V. J. Cardone, J. G. Greenwood, and M. A. Cane (1997), The recent increase in North Atlantic wave heights, *J. Clim.*, *10*, 2107–2113.

Nakamura, H., T. Izumi, and T. Sampe (2002), Interannual and decadal modulations recently observed in the Pacific Storm track activity and east Asian winter monsoon, *J. Clim.*, *15*, 1855–1874.

Snodgrass, F. E., G. W. Groves, K. F. Hasselmann, G. R. Miller, W. H. Munk, and W. H. Powers (1966), Propagation of Ocean swell across the Pacific, *Philos. Trans. R. Soc. London A*, *259*, 431–497.

Wang, B., and J. C. L. Chan (2002), How strong ENSO events affect tropical storm activity over the western North Pacific, *J, Clim.*, *15*, 1643–1658.

Wang, X. L., and V. R. Swail (2001), Changes of extreme wave heights in Northern Hemisphere Oceans and related atmospheric circulation regimes, *J. Clim.*, *14*, 2204–2221.

Whitaker, L. M., and L. H. Horn (1984), Northern Hemisphere extratropical cyclone activity for four mid-season months, *J. Climatol.*, *4*, 297–310.

S. Iizuka, S. I. Iwasaki, T. Matsuura, W. Sasaki, and I. Watabe, National Research Institute for Earth Science and Disaster Prevention, Tenno-dai 3-1, Tsukuba, Ibaraki, Japan. (wsasaki@bosai.go.jp)